

Redox Transformations in Ferrimyoglobin Induced By Radiation-generated Free Radicals in Aqueous Solution*

(Received for publication, June 11, 1981)

Kevin D. Whitburn, James J. Shieh, Robin M. Sellers‡, and Morton Z. Hoffman

From the Department of Chemistry, Boston University, Boston, Massachusetts 02215

Irwin A. Taub

From the Food Engineering Laboratory, United States Army Natick Research and Development Laboratories, Natick, Massachusetts 01760

The interactions of radiation-generated $\cdot\text{OH}$ and e_{aq}^- with ferrimyoglobin in aqueous solution at pH 7.3 have been studied as functions of dose, dose-rate, and the presence of oxygen. Correction for postirradiation thermal processes allows for radiation-induced compositional changes to be separately studied. In deaerated solution, radiolysis induces conversions to the deoxy- and ferriperoxide derivatives of myoglobin. Aeration of irradiated solutions quantitatively converts the deoxy form to oxymyoglobin. Only ferrimyoglobin peroxide is generated upon irradiation of N_2O -saturated solutions of ferrimyoglobin containing oxygen. With both $\cdot\text{OH}$ and e_{aq}^- as precursor radicals, a radiolysis steady state is attained at moderate doses involving the ferri-, and ferriperoxide forms of myoglobin. The actual composition depends on the radical system under consideration. These results are interpreted in terms of radiation-induced 1-eq redox conversions among the myoglobin prosthetic forms. Radical attack on the hemoprotein that does not lead to such conversions modifies the globin moiety through dimerization and disproportionation processes. Independence of $G(\text{ferri} \rightarrow \text{deoxy})$ and $G(\text{dimer})$ over an enormous variation in dose-rate indicates that the inherent reduction and bimolecular processes do not compete. Protein-mediated reduction in the ferri \rightarrow deoxy process induced by $\cdot\text{OH}$ radicals is established. The yield of ferrimyoglobin peroxide in the oxygenated $\cdot\text{OH}$ system is beyond that accountable by thermal interaction of H_2O_2 with the ferri substrate. The extra yield results from a diversion of intermediates away from reductive conversion reactions and toward peroxide production by the interaction of oxygen. A basis for the clarification of earlier controversies about the radiation chemistry of myoglobin is offered, along with insights into the nature of protein-mediated redox processes in metalloproteins.

One-equivalent redox reactions involving hemoproteins have been actively investigated using the techniques of radiation chemistry; reactions most studied have been cytochrome(III) *c* and ferrihemoglobin with radiation-generated

* This research was supported by the United States Army through Contract DAAG60-79-C-0005 to Boston University. The costs of publication of this article were defrayed in part by the payment of page charges. This article must therefore be hereby marked "advertisement" in accordance with 18 U.S.C. Section 1734 solely to indicate this fact.

‡ Present address, Central Electricity Generating Board, Berkeley, Gloucestershire, England.

free radicals (1-9). The issue of globin-mediated reductive transfer in metalloproteins has been addressed by several authors, and there is reasonable agreement that for the cytochrome(III) *c* + e_{aq}^- system some indirect reduction is likely, in addition to direct interaction at the ferriheme site (1, 3, 4, 9). The nature of the partitioning between direct and indirect reductive pathways in the interaction of e_{aq}^- with ferrimyoglobin and ferriHb¹ has remained less clear (5, 6). Although intermediate processes in the reaction of e_{aq}^- with ferriMb (7), and of $\cdot\text{OH}$ with ferriHb (5) have been investigated, a rigorously quantitative study of primary radical interactions with ferriMb, with a focus on mechanism, has not been reported.

Previous studies spanning the past 25 years on the radiation chemistry of meat extracts and myoglobin solutions collectively show that the effects of ionizing radiation are not fully understood. There is reasonable consensus that ferriMb is reduced by radiolysis in aqueous solution, but the interpretation of the spectrum of the oxymyoglobin-like product has remained a point of contention. While some authors believe that the red, aerated product is oxymyoglobin (10, 11), others claim it is merely a spectrally similar material (13, 15). A recent account of the situation appears in the introduction of a paper by Kamarei *et al.* (16).

The product identity issue has been complicated in the previous qualitative studies of spectral changes in aerated solution because the oxy and ferriperoxide forms of myoglobin have similar absorbance maxima in the visible region. Moreover, in most of the earlier reports (10, 12, 15-17), the peroxide form has not been included in the evaluation of products from the radiolysis of ferriMb. This omission has been crucial, since this form may be readily generated by the reaction of ferriMb with H_2O_2 (18, 19), an unavoidable product of the radiolysis of aqueous solutions. The importance of the ferriperoxide form as a product component was conclusively shown by Bernofsky *et al.* (14) who found that it could be generated by simply adding irradiated water to ferriMb solution. This feature was confirmed by Giddings and Markakis (20) who further showed that the peroxide could be reduced back to ferriMb by addition of $\text{Fe}(\text{CN})_6^{4-}$.

In addition to disagreement as to the nature of the red product, some disagreement exists about the nature of the primary radicals that induce the observed color changes. While Tappel (10) and Bernofsky *et al.* (14) have proposed that $\cdot\text{OH}$ radicals are the likely initiators, Satterlee *et al.* (17) more recently have claimed that $\cdot\text{OH}$ is an insignificant participant, thereby focusing on the e_{aq}^- species. The negligible $\cdot\text{OH}$ -induced reduction of ferriMb recently reported by

¹ The abbreviations used are: ferriHb, ferrihemoglobin; ferriMb, ferrimyoglobin.

Van Leeuwen *et al.* (8) lends support to Satterlee's view. Giddings and Markakis (20), furthermore, cite O_2^- as a possible initiator of oxymyoglobin formation in ferriMb radiolysis. Regardless of these disputed issues, there is conclusive evidence that radiolysis of myoglobin at moderate doses induces changes in the globin structure, while leaving the heme group intact (15, 21). At high doses, the porphyrin structure of the heme is ultimately degraded (12, 16).

As part of our research on the radiation-preservation of meat (22), we have quantitatively studied the interaction of selected free radicals with myoglobin in aqueous solution using the pulse and continuous radiolysis techniques. The focus of this report is on the reactions of $\cdot\text{OH}$ and e_{aq}^- with purified ferriMb in aqueous solution, investigated as functions of dose, dose-rate, and the presence of oxygen. In the context of the radiation chemistry of myoglobin, the systematic and quantitative approach adopted in this study offers considerable clarification of the disputed issues, in addition to providing background to the mechanisms of radiation-damage processes. Insight into the mechanism of protein-mediated redox processes is also developed.

EXPERIMENTAL PROCEDURES

Materials—Bovine myoglobin was obtained from fresh beef muscle. The method used for isolation and purification of oxymyoglobin followed literature techniques (23, 24). The method involved the homogenization of 350 g of the tissue with 700 ml of cold water into a slurry followed by centrifugation. The water extract was further fractionated, first with ethanol and then with a solution containing lead subacetate and zinc acetate. The resulting solution was chromatographed on DEAE-cellulose and Sephadex G-75 columns. The purified MbO_2 produced only one band upon gel electrophoresis (25); 7% polyacrylamide gel in glycine-Tris buffer at pH 8.3 was used. FerriMb was produced by oxidation of the pure MbO_2 by a 20% molar excess of $\text{K}_3\text{Fe}(\text{CN})_6$ and removed by dialysis and Sephadex G-75 column chromatography. The deoxy form was generated by reduction of ferriMb in deaerated solution (Ar-purged) by a 200-fold molar excess of $\text{Na}_2\text{S}_2\text{O}_4$. Ferrimyoglobin peroxide was produced by addition of excess H_2O_2 to ferriMb in the ratio 6:1 at pH 7.3 (18); a characteristic greenish color developed quickly upon mixing. At this pH the peroxide is present as a mixture of two forms, with the green acidic form dominating over the red basic form (19). This form of myoglobin has been referenced in the early literature as "ferrylmyoglobin" (14, 20), and is formally designated as FeO^{2+} (26) or $\text{Mb}(\text{IV})$ (27), which emphasizes that the heme center is 1 eq higher in its oxidation state than is ferriMb. Except where indicated, the myoglobin in all the solutions irradiated in this study was in the ferriMb form to the extent of >96%.

All other chemicals were of the highest analytical grade available and were used without further purification.

Procedures—Solutions for irradiation were prepared from distilled water purified by passage through a Millipore Purification Train (resistance >18 M Ω). All solutions used in this study were buffered with phosphate (0.01 M) at pH 7.3. The solution vessels were 10-mm Spectrosil spectrophotometer cuvettes, each with a long graded-seal neck attached to allow for an hermetic seal with a rubber septum. The solutions were deaerated by purging with Ar or N_2O at 2 °C using fine syringe needles through the septa for the gas flow inlet and outlet. The Ar and N_2O were scrubbed of oxygen by passage through alkaline pyrogallol solution and an Oxisorb (Messer Griesheim) cartridge, respectively.

Radiation Sources—Continuous radiolyses were performed using ^{60}Co and ^{137}Cs γ -sources. The dose rates, determined by standard Fricke dosimetry, were 6.1 (+ 0.4) and 14.9 (+ 3.0) krad min^{-1} , respectively; the values added in parentheses are the absolute doses deposited during the down-up motion of the sample elevator in the irradiators. Pulse radiolysis with optical transient absorption detection was carried out using a Febetron 705 pulse generator with associated electronics (28) having a time resolution of 0.5 μs . Where indicated, a 10-MeV LINAC source was used. The radiation dose per pulse was measured by SCN^- and pulse-Fricke dosimetry. All irradiations were performed at ambient temperature, 22 (\pm 2) °C. The radiation facilities at the United States Army Natick Research and Development Laboratories, Natick, MA were used.

Generation of Radicals—In the high energy radiolysis of aqueous solutions, the following primary species are generated: e_{aq}^- (2.8), $\cdot\text{OH}$ (2.8), $\text{H}\cdot$ (0.6), H_2O_2 (0.7). The G values or molecular yields/100 eV of energy absorbed appear in parentheses. In the presence of N_2O , e_{aq}^- is readily converted to $\cdot\text{OH}$ radicals (29); $G(\cdot\text{OH})$ becomes 5.6 under this condition. The presence of *tert*-butyl alcohol in Ar-purged solutions converts the $\cdot\text{OH}$ radical to the unreactive $\cdot\text{CH}_2(\text{CH}_3)_2\text{COH}$ radical, via an H atom abstraction process, leaving e_{aq}^- as the dominant reactive species.

Analyses—Preirradiated solutions were spectrophotometrically analyzed in the 450–700-nm region on a Cary 118 spectrophotometer. Immediately after radiolysis, the solutions were repeatedly scanned in this region by means of a repetitive scan control unit. In all but a few cases, spectral measurements were initiated within 3 min of the radiolysis (continuous or pulse). For the postirradiation kinetic measurements, zero time was taken as the midpoint of the radiolysis duration, and analysis times were taken at the 545-nm point of the repetitive scans. Facile numerical computation for composition analyses, with absorbance data as input, was achieved using a Hewlett-Packard 9830A programmable calculator with printer and tape storage capability.

Chromatography on unirradiated controls and postirradiated sample solutions were performed on Sephadex G-100 columns. Each solution was applied to a column (2.2 \times 100 cm) and eluted with 0.01 M phosphate buffer at pH 7.4. The flow rate was 0.2 ml min^{-1} . Spectrophotometric detection of the eluant fractions was performed using a Uvicord UV monitor at 280 nm. Blue dextran, alcohol dehydrogenase, and bovine serum albumin were used as molecular weight standards.

RESULTS

Shown in Fig. 1 are the absorption spectra in the visible region to the red of the Soret bands of the ferri-, deoxy-, oxy-, and ferriperoxide forms of myoglobin at pH 7.3; the ϵ values are based on $\epsilon_{580}(\text{MbO}_2) = 1.46 \times 10^4 \text{ M}^{-1} \text{ cm}^{-1}$ (23). Particularly notable are the similar positions of the absorbance maxima of the MbO_2 and ferriperoxide derivatives in the 545- and 580-nm regions.

Throughout this study, the spectral changes induced upon irradiation of ferriMb in deaerated solution show a depletion of the characteristic ferri peaks accompanied by absorbance growth in the 250–610-nm region regardless of the nature of the precursor radical. After both steady state and pulsed irradiation, there is a slow thermal regeneration of ferriMb absorbance with the concomitant loss of the absorbance previously generated. This feature is illustrated in Fig. 2 for a N_2O -saturated, 30.7 μM ferriMb solution irradiated to a dose of 20.5 krad, for which isosbestic integrity at 465, 519, and 611 nm is maintained over the duration of the thermal process. In most cases, the thermal process was followed as a function of time for 0.5–1 h. With the ϵ values known from Fig. 1 for each

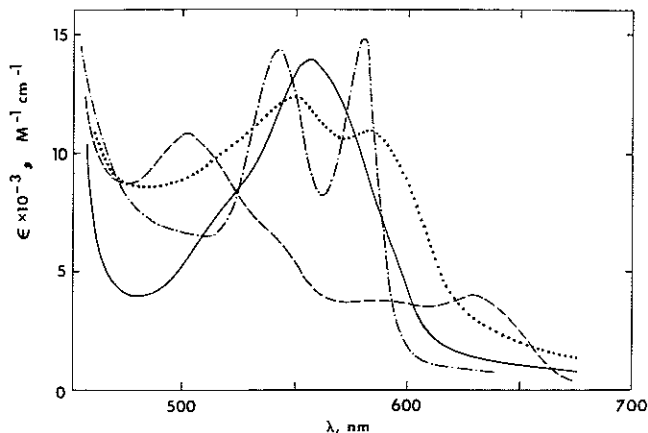
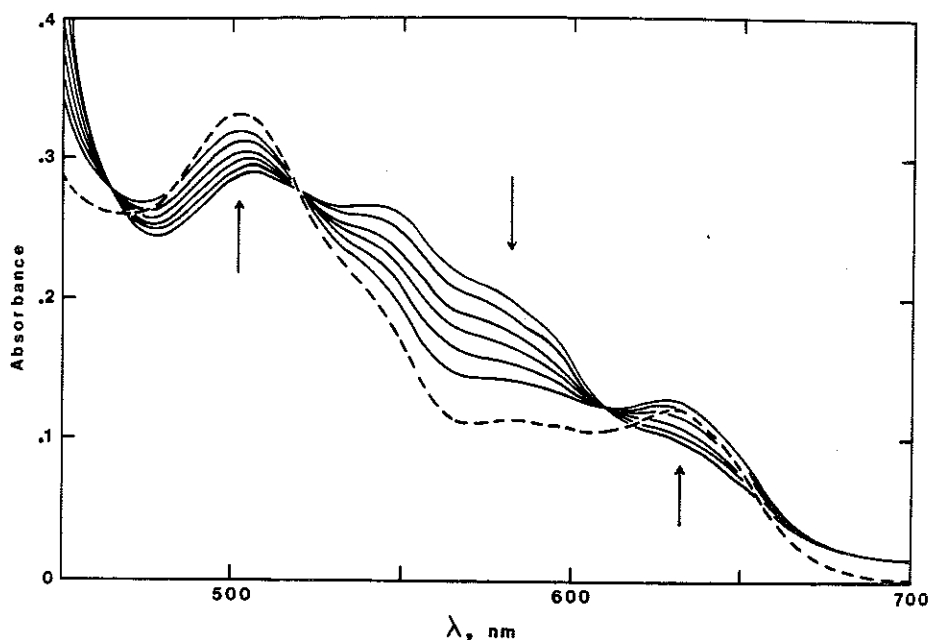


FIG. 1. Absorption spectra of myoglobin derivatives to the red of the Soret bands at pH 7.3. Ferrimyoglobin, ---; deoxy-myoglobin, —; ferri-myoglobin peroxide, ...; oxymyoglobin, -.-.

FIG. 2. Spectral changes induced by 20.5 krad of γ -radiation in an N_2O -saturated $30.7 \mu M$ ferriMb solution. Before radiolysis ---; after radiolysis —, measured 3.4, 6.4, 19.6, 34.0, 59.0 min after initial time of radiolysis. Arrows indicate direction of postirradiation absorbance changes.



relevant myoglobin derivative, the observed spectral changes were analyzed in terms of component composition. Accurate compositional data of ferri, deoxy, and peroxide forms of myoglobin were determined from absorbance measurements at three chosen wavelengths (500, 560, and 590 nm) by the solving of simultaneous equations based on Beer's Law. The constancy of the calculated total myoglobin concentration, both before the radiolysis and during the postirradiation thermal process, is consistent with there being insignificant quantities of absorbing species in solution other than those analyzed. This observation held true, within 3%, for both of the primary radical systems over the dose ranges studied.

The spectral-based composition analysis reveals that radiolysis in deaerated solution induces a conversion of ferriMb to both Mb and ferriperoxide, and that the thermal regeneration of ferriMb involves both of these product forms. These features are illustrated in Fig. 3, where the compositional changes of the components with time, derived from the absorbance data of Fig. 2, are shown. In order to examine the radiation-induced compositional changes, component compositions were extrapolated linearly through the early portion of the thermal process (through <15% of the total thermal change) back to zero time. In the example illustrated in Fig. 3, the $30.7 \mu M$ solution, initially >98% ferriMb, is converted into a mixture of 53% ferriMb, 18% Mb, and 29% Mb(IV).

Initial rates of ferriMb regeneration and of Mb and ferriperoxide loss are shown in Table I along with the concentrations at zero time of the two radiolysis products. The initial rate data, measured as micromolar per min, are derived directly from composition *versus* time plots (illustrated in Fig. 3) for both $\cdot OH$ and e_{aq}^- as precursor radicals. In cases where Mb is in limiting concentration, there is a very slow ($t_{1/2} \sim 1$ –2 h) residual conversion of ferriperoxide to ferri-like material. This complex process has been previously described (19, 27).

Reaction of $\cdot OH + FerriMb$ — N_2O -saturated solutions containing $30 (\pm 2) \mu M$ ferriMb were γ -irradiated in the dose range 3.1–55.2 krad. Loss of ferriMb is accompanied by formation of both Mb and ferriperoxide. The radiation-induced compositional changes corrected for the postirradiation process are shown as a function of dose in Fig. 4a. After ~ 30 krad, or a dose/ μM of myoglobin of ~ 1 krad/ μM , the solution composition becomes essentially independent of dose for further moderate dose increases, remaining 18% Mb, 38% ferriperoxide,

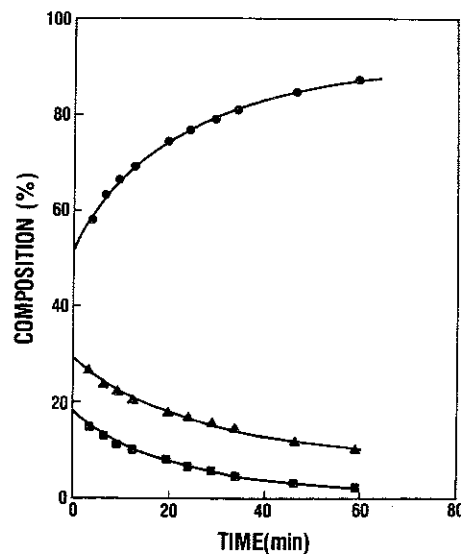


FIG. 3. Composition changes of ferriMb (●), Mb (■), and ferriperoxide (▲) as a function of time after radiolysis. Solution initially >98% in the ferriMb form; concentration $30.7 \mu M$, dose 20.5 krad, N_2O -saturated, pH 7.3.

and 44% ferriMb. As seen in Table II, the same steady state composition is approached for solutions initially containing 36 or 100% Mb(IV). Significantly larger doses are required to reach the radiolysis steady state as the proportion of ferriperoxide initially present is increased. The observed $G(Mb)$ and $G(Mb(IV))$ values are plotted against dose in Fig. 4b. An inverse relationship between $G(Mb)$ and dose holds for dose values above ~ 20 krad as a consequence of the steady state nature of the solution composition in this region. This relationship is apparent in the reciprocal plot included in Fig. 4b. In the limit of zero dose, $G(Mb) = 1.4 (\pm 0.2)$ and $G(Mb(IV)) = 0.7 (\pm 0.1)$. The likely participation of H atoms in the reductive process was demonstrated for an N_2O -saturated, $33 \mu M$ ferriMb solution containing $0.05 M$ *tert*-butyl alcohol that was γ -irradiated to a dose of 20 krad. The observed $G(Mb)$ of ~ 0.05 is attributed to H atom reaction with the ferriMb. Consequently, the reductive conversions obtained in N_2O -saturated solutions of this substrate may be considered a

TABLE I
Initial rates of the thermal process following γ -radiolysis at pH 7.3 in deaerated solution

Dose	[ferriMb] ₀	[Mb] ^a	[Mb(IV)] ^a	R _{ferriMb}	R _{Mb}	R _{Mb(IV)}
krad	μM	μM			$\mu\text{M min}^{-1}$	
4.1 ^b	32.3	4.3	2.1	0.13	0.08	0.06
5.2 ^b	29.8	2.8	2.9	0.16	0.09	0.08
10.9 ^b	28.0	5.0	4.9	0.23	0.12	0.11
12.0 ^b	29.1	4.3	5.5	0.37	0.14	0.22
31.5 ^b	30.7	5.4	9.0	0.62	0.26	0.30
42.7 ^b	31.1	5.6	10.3	0.65	0.28	0.33
41.7 ^b	14.1	1.3	8.3	0.25	0.07	0.16
41.7 ^b	15.7	2.6	6.2	0.36	0.07	0.28
41.7 ^b	31.1	5.4	11.3	1.02	0.44	0.57
41.2 ^b	39.0	6.8	13.2	1.14	0.48	0.60
5.4 ^c	35.0	8.6	2.5	0.23	0.14	0.13
14.9 ^c	23.6	12.2	3.0	0.52	0.15	0.35
13.4 ^c	37.0	17.6	5.0	0.72	0.48	0.18
15.7 ^c	39.8	22.2	1.0	0.19	0.18	0.03
25.0 ^c	36.5	23.7	3.1	0.79	0.61	0.20
37.6 ^c	37.9	24.5	4.2	0.98	0.65	0.26

^a Extrapolated to midpoint of radiolysis duration.

^b N₂O-saturated.

^c Ar-purged, 0.1 M *tert*-butyl alcohol.

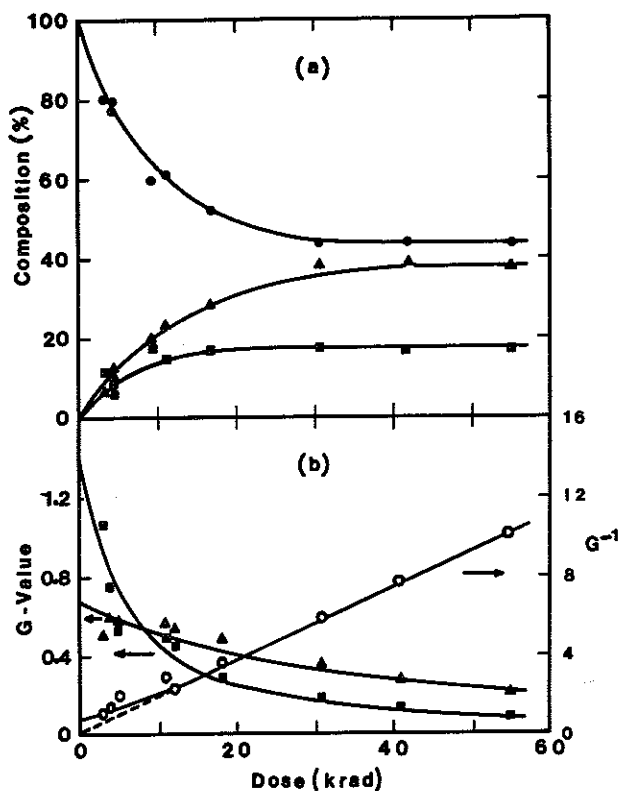


FIG. 4. Composition changes and G-values as functions of dose. *a*, γ -induced composition changes as a function of dose. *b*, left ordinate: G values of γ -induced ferriMb conversions to Mb and ferriperoxide as a function of dose. Right ordinate: reciprocal of the G (ferri-Mb \rightarrow Mb) values as a function of dose (O). FerriMb (●), Mb (■), ferriperoxide (▲). Solutions N₂O-saturated, 30 (\pm 2) μM in myoglobin.

composite of $\cdot\text{OH}$ and $\text{H}\cdot$ reactivity, with $\cdot\text{OH}$ clearly dominating ($G(\cdot\text{OH}) \approx 10G(\cdot\text{H})$).

An N₂O-saturated 27.5 μM ferriMb solution, γ -irradiated to 14.9 krad, was thoroughly aerated after following the deaerated postirradiation process for 6 min. Upon aeration, the Mb product quantitatively converts to MbO₂, which then continues to undergo the thermal reaction at a similar rate. Composition analysis was based on the MbO₂, ferriMb, and ferri-

peroxide forms from absorbance measurements at 490, 560, and 580 nm. When N₂O-saturated solutions of ferriMb (26 \pm 2 μM) are exposed to γ -rays in the presence of 0.3 mM O₂, there is no reductive conversion of ferriMb to MbO₂; ferriperoxide is the only product. This feature has been previously reported by Giddings and Markakis (20). The compositional changes are shown as a function of dose over the range 3.9–5.5 krad in Fig. 5*a*. After about 20 krad, the percentages of ferriMb and the peroxide become independent of dose for further moderate increases, remaining essentially constant at 33% ferriMb and 67% ferriperoxide. The observed process after irradiation in oxygenated solution has a $t_{1/2} \sim \text{h}$, consistent with the complex ferriperoxide conversion to ferri-like material (19, 27) under conditions in which no reduced form of ferriMb is present. The observed $G(\text{Mb(IV)})$ values are plotted against dose in Fig. 5*b*. In the limit of zero dose, $G(\text{Mb(IV)}) = 1.5 (\pm 0.2)$, which is significantly greater than that obtained for the radiolysis of deaerated solutions.

Upon delivery of 3.1 krad to an N₂O-saturated, 32 μM ferriMb solution in a single LINAC pulse, the observed

TABLE II
Radiation-induced composition changes as a function of initial composition for N₂O-saturated myoglobin solutions at pH 7.3

Normalized dose ^a	Initial composition ^b			Composition after radiolysis ^b		
	FerriMb	Mb	Mb(IV)	FerriMb	Mb	Mb(IV)
krad μM^{-1}		%			%	
1.34	100	0	0	44	18	38
2.66	100	0	0	44	17	39
3.98	100	0	0	45	17	38
1.48	64	0	36	34	10	56
2.80	63	0	37	40	14	46
4.41	64	0	36	43	18	39
1.62	0	0	100	28	4	68
2.96	0	0	100	31	10	59

^a Dose per μM of myoglobin.

^b Composition error: 2–5%.

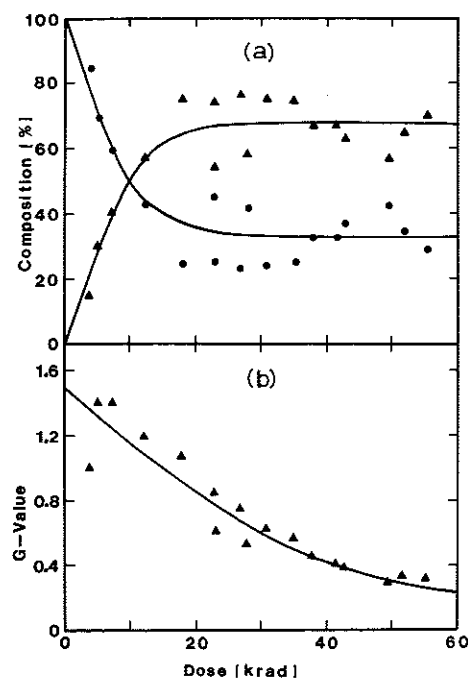
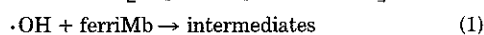


FIG. 5. Composition changes and G-values as functions of dose. *a*, γ -induced composition changes as a function of dose. *b*, G values of γ -induced conversion of ferriMb to ferriperoxide as a function of dose. Solutions 26 (\pm 2) μM in myoglobin, N₂O-saturated, 0.3 mM in O₂ at pH 7.3. FerriMb (●), ferriperoxide (▲).

$G(\text{Mb})$, corrected for the postirradiation process, was 0.5 (± 0.1), which is significantly less than that obtained by γ -radiolysis to the same concentration-normalized dose. In order to estimate the loss of $\cdot\text{OH}$ radicals by bimolecular self-recombination under the pulse condition, a value of $k(\cdot\text{OH} + \text{ferriMb})$ was estimated by varying $[\text{ferriMb}]$ between 18 and 52 μM in a pulse radiolysis experiment monitored at 560 nm; a value of $\sim 8 \times 10^9 \text{ M}^{-1} \text{ s}^{-1}$ was obtained. To a reasonable approximation, expression (A) relates the effect of the competition between reactions 1 and 2 on the observed G value for the $\text{ferriMb} \rightarrow \text{Mb}$ process. $G(\text{pulse})$ is the yield of Mb for the pulse experiment in the absence of the competition. This term is modified by the rate-ratio term for the fraction of $\cdot\text{OH}$ actually interacting with the substrate. By suitable rearrangement and substitution using $2k_2 \approx 1 \times 10^{10} \text{ M}^{-1} \text{ s}^{-1}$ (30) and $[\cdot\text{OH}] \approx G(\cdot\text{OH}) \times \text{dose}$ (krad), we derive

$$G(\text{obsd}) \approx G(\text{pulse}) \left[\frac{k_1 [\text{ferriMb}]}{k_1 [\text{ferriMb}] + 2k_2 [\cdot\text{OH}]} \right] \quad (\text{A})$$



$G(\text{pulse}) \approx 0.8$ (± 0.1).

This dose-rate analysis indicates that the $\cdot\text{OH}$ -induced $\text{ferriMb} \rightarrow \text{Mb}$ conversion is essentially independent of transient concentration over an enormous range. This independence was confirmed in a separate experiment in which N_2O -saturated solutions of 0.49 mM ferriMb were multiply pulsed (LINAC source) at doses of 5.1 and 0.64 krad/pulse to a total dose of 51 and 48 krad, respectively. Under these conditions, where $>95\%$ of the $\cdot\text{OH}$ radicals react with the substrate, $G(\text{Mb})$ is 0.9 (± 0.1), independent of the dose/pulse.

Column chromatographic analysis (Sephadex G-100) of pulsed (67 krad, 4.2 krad/pulse, LINAC source) and γ -irradiated (61 krad, 6.1 krad min^{-1}) N_2O -saturated ferriMb (0.49 mM) solutions shows evidence of dimer formation (Fig. 6); $G(\text{dimer}) = 0.5$ (± 0.05), independent of the immense variation in dose-rate. As expected, an increase in dimer production at the expense of monomer is observed with increasing dose. At concentration-normalized doses greater than $\sim 1 \text{ krad } \mu\text{M}^{-1}$, trimer formation becomes apparent. The generation of dimer material in the γ -radiolysis of aqueous ferriMb has been previously reported (21).

The transient processes induced by $\cdot\text{OH}$ reaction with ferriMb were studied by pulse radiolysis of N_2O -saturated solutions containing 30–60 μM myoglobin. The spectral changes produced within 3 μs , 80 μs , and 400 ms of the pulse are shown in Fig. 7. Two separate processes are observed in the 300–325-nm region. The faster one is a dose-dependent absorbance growth in the Soret region within 0.5 ms of the pulse, a simple second order plot of which, monitored at 430 nm, shows linearity over two half-lives (Fig. 8). A slower process, characterized by small absorbance losses in the 320- and 470-nm regions, occurs within 100 ms of the pulse; no meaningful kinetic analysis was attainable. In the $\cdot\text{OH} + \text{ferriMb}$ system, Clement *et al.* (5) observed transient processes on the same time scale as those just described. The faster process was reported as first order ($k \sim 10^4 \text{ s}^{-1}$) and interpreted as a reducing-equivalent migration from a globin radical to a heme iron. Although the kinetics of our faster process appear reasonably second order, the ability of added O_2 to scavenge reducing globin radicals leads us to concede that there may be some first order character in the observed transient change on this time scale that may be more discernible at shorter wavelengths. Reliable kinetics in the 300-nm region were unattainable in this highly absorbing substrate system, however.

Reaction of $e_{aq}^- + \text{FerriMb}$ —Ar-purged solutions containing

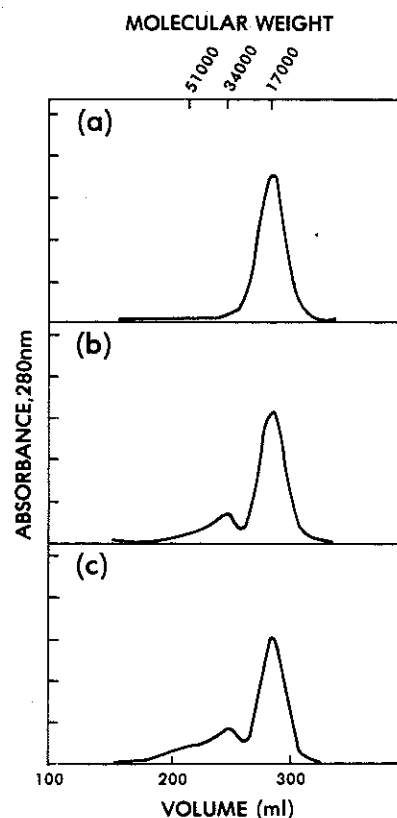


FIG. 6. Chromatography on Sephadex G-100 of unirradiated and irradiated solutions of ferriMb (0.49 mM), saturated with N_2O at pH 7.4. a, control; b, γ -irradiated, 61 krad; c, pulse-irradiated, 67 krad. Each ordinate interval corresponds to 0.2 absorbance unit at 280 nm.

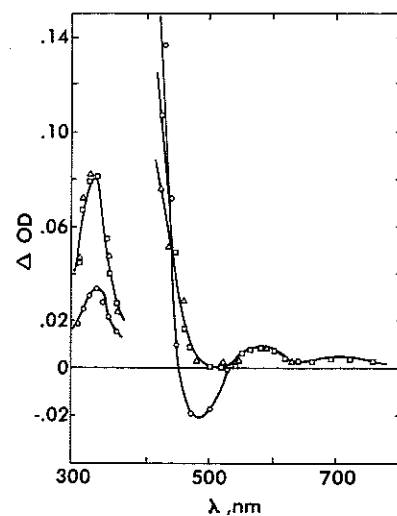


FIG. 7. Spectral changes resulting from pulse radiolysis of N_2O -saturated ferriMb solution (60 μM , pH 7.3, dose 1.6 krad pulse^{-1}) measured 3 μs (Δ), 80 μs (\square), and 400 ms (\circ) after the pulse.

38 (± 2) μM ferriMb and 0.1 M *tert*-butyl alcohol were γ -irradiated in the dose range 1.6–69.7 krad. The induced compositional changes, corrected for the postirradiation process, are shown as a function of dose in Fig. 9a. As with the $\cdot\text{OH}$ radical, loss of ferriMb is accompanied by the formation of both Mb and ferriperoxide. A plateau region of composition change is also attained after a dose of ~ 35 krad. The solution composition in the steady state region is 64% Mb, 12% ferriperoxide, and 24% ferriMb , markedly different from that ex-

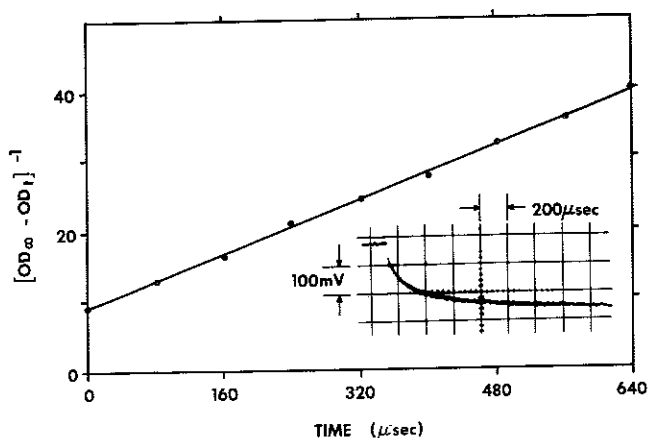


FIG. 8. Kinetic trace and simple second-order plot of the absorbance change at 430 nm in pulsed (1.6 krad) N_2O -saturated ferriMb solution ($30 \mu M$, pH 7.3).

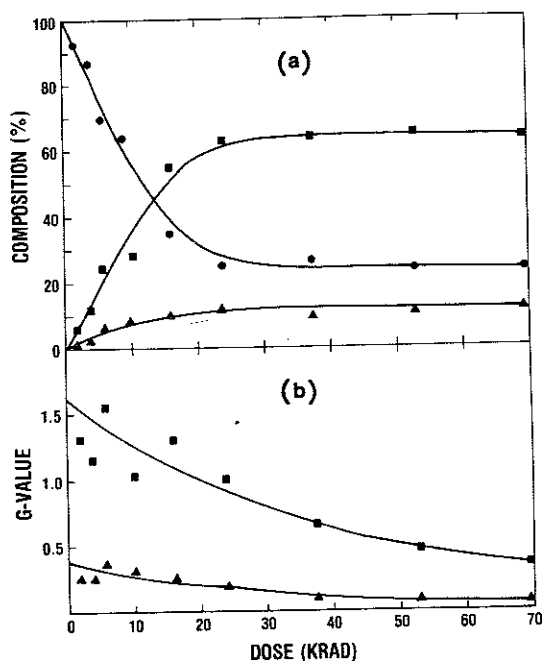


FIG. 9. Composition changes and G -values as functions of dose. *a*, γ -induced composition changes as a function of dose. *b*, G values of γ -induced ferriMb conversions to Mb and ferriperoxide as a function of dose. FerriMb (●), Mb (■), ferriperoxide (▲). Solutions Ar-purged, $38 (\pm 2) \mu M$ in myoglobin, 0.1 M in *tert*-butyl alcohol at pH 7.3.

hibited by $\cdot OH$ radicals. The percentages attained after γ -radiolysis of solutions $22 (\pm 1) \mu M$ in myoglobin and initially 53–63% in ferriperoxide are compared with the radiolysis of a solution of 100% ferriMb in Table III. The same steady state is approached, but at significantly higher doses, which clearly involves the participation of both the ferriMb \rightarrow Mb and the ferriperoxide \rightarrow ferriMb conversions. The observed $G(Mb)$ and $G(Mb(IV))$ values are shown as functions of dose in Fig. 9*b* where, in the zero-dose limit, $G(Mb) = 1.6 (\pm 0.2)$ and $G(Mb(IV)) = 0.4 (\pm 0.1)$.

Pulse radiolysis of Ar-purged ferriMb solutions (40 – $80 \mu M$) containing 0.1 M *tert*-butyl alcohol shows rapid heme(III) reduction; transient absorbance characteristic of Mb in the 450–650-nm region is apparent after the primary reaction. A value of $k(e_{aq}^- + \text{ferriMb}) = 3.1 (\pm 0.5) \times 10^{10} M^{-1} s^{-1}$ was obtained from the variation of [ferriMb] (18 – $53 \mu M$) at constant dose. A process leading to slight absorbance changes in

the above spectral region follows with $t_{1/2} \sim 100 \mu s$. These spectral observations, shown in Fig. 10, have been previously reported and interpreted (6, 7). Based on the absorbance changes at 560 nm (where $\Delta\epsilon \approx 1.02 \times 10^4 M^{-1} cm^{-1}$) measured 0.5 msec after a 1.1-krad pulse, $G(\text{ferriMb} \rightarrow Mb)$ is $1.3 (\pm 0.1)$. When this value is corrected for e_{aq}^- self-recombination and compared with the continuous radiolysis G value of ~ 1.6 , it is apparent that the e_{aq}^- -induced yield of Mb is independent of dose-rate over an enormous range, which is analogous to the results obtained in the $\cdot OH$ system.

DISCUSSION

The Post-irradiation Process—Although regeneration of the substrate absorbance has been previously observed at room temperature after the radiolysis of ferriMb solutions

TABLE III

Radiation-induced composition changes as a function of initial composition for Ar-purged myoglobin solutions containing 0.1 M *tert*-butyl alcohol at pH 7.3

Normalized dose ^a	Initial composition ^b			Composition after radiolysis ^b		
	FerriMb	Mb	Mb(IV)	FerriMb	Mb	Mb(IV)
$krad \mu M^{-1}$		%			%	
0.63	100	0	0	25	64	11
1.39	100	0	0	24	64	12
1.02	63	1	36	18	61	21
1.48	53	0	47	22	60	17
2.00	56	1	43	30	58	12

^a Dose per μM of myoglobin.

^b Composition error: 2–5%.

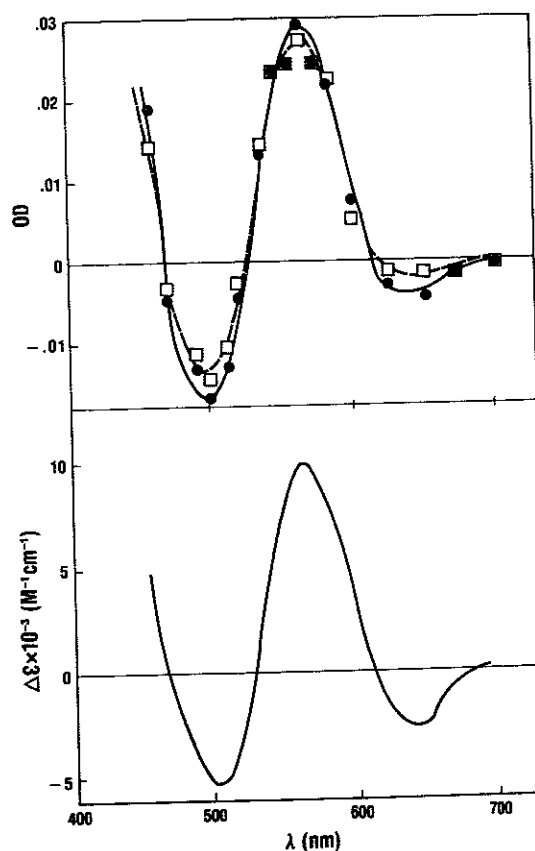
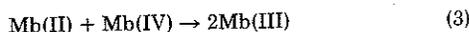


FIG. 10. Comparison of transient absorption spectra with known difference spectrum. *Upper*, absorption spectra measured at end of pulse (□) and 500 μs after the pulse (●) of Ar-purged ferrimyoglobin solution ($56 \mu M$) containing 0.1 M *tert*-butyl alcohol at pH 7.3. *Lower*, difference spectrum of ferriMb and deoxyMb.

(14), no mechanistic explanation has been offered. The quantitative data obtained for this process in this investigation enables a mechanistic interpretation to be made. From Table I, it is apparent that the initial rate of ferriMb formation is equal to the sum of the initial rates of decay of the Mb and Mb(IV) radiolysis products. Since this reaction involves myoglobin prosthetic forms that are formally 1 eq below and above, respectively, the Fe(III) redox state in ferriMb, we propose that the dominant post-irradiation process



may be formally considered as a synproportionation reaction. An estimate of k_3 can be made from a plot of $R_{\text{ferriMb}}/[\text{Mb}]$ as a function of [ferriperoxide] as shown in Fig. 11. This plot uses the data from both the $\cdot\text{OH}$ and e_{aq}^- precursor systems in Table I. Division of the derived slope by two, inasmuch as two ferriMb molecules are formed for each reactant pair, gives $k_3 = 1.2 (\pm 0.3) \times 10^2 \text{ M}^{-1}\text{s}^{-1}$ at pH 7.3. In the absence of reduced heme products, the ferriperoxide undergoes slow conversion to ferriMb-like material through a complex mechanism (19, 27).

Radiolysis Stoichiometry—The detectable radiolysis products induced by $\cdot\text{OH}/\text{H}\cdot$ in N_2O -saturated solutions account for a ferriMb conversion yield of $G(\text{Mb}) + 2 G(\text{dimer}) \approx 2.4$, significantly below the total radical yield of 6.2. From a study of the spectra of irradiated myoglobin solutions (21), it has been reported that there is no discernible spectral difference among the chromatographically separated monomer, dimer, and polymer product fractions. Upon removal of the heme group from the product material, it was further shown that the heme had suffered no measurable spectral change. Gel electrophoresis of the corresponding apomyoglobins (*i.e.* heme-free) indicated that the chemical alterations were centered on the globin portion of the macromolecule (15). We propose, therefore, that the remaining $G \approx 3.8$ of the total radical yield is accountable by oxidized products of globin radical disproportionation (unsaturation or OH-substitution) processes for which G (oxidation) ≈ 1.9 . Accompanying the production of oxidized monomeric protein from the free radical precursors must be regeneration of unmodified ferriMb. Oxidation at a single site within the monomeric metalloprotein would not be spectrally significant in the observed visible region, unless key heme sites were involved. Our spectral

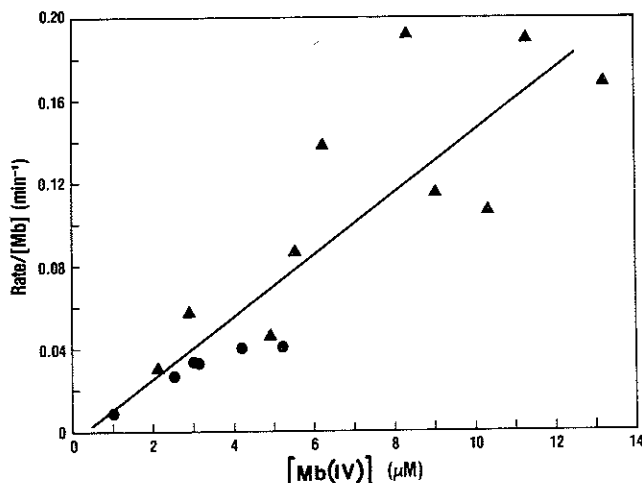
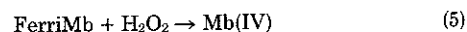
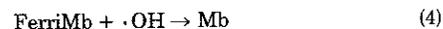


FIG. 11. Rate of thermal regeneration of ferriMb divided by deoxyMb concentration, as a function of ferriperoxide concentration; data extrapolated to the midpoint of the radiolysis duration. $\cdot\text{OH}$ data, \blacktriangle : $30 (\pm 2) \mu\text{M}$ in myoglobin, 4–43 krad; e_{aq}^- data, \bullet : $38 (\pm 2) \mu\text{M}$ in myoglobin, 14–38 krad.

analyses are consistent with nonheme sites of chemical modification.

Radiolysis Processes—The γ -induced changes in myoglobin composition as functions of dose (Figs. 4, 5, and 9) behave in a manner analogous to those of a first order approach to equilibrium in a kinetic system. In this context, however, the equilibrium is a radiolysis steady state involving three forms of the myoglobin prosthetic group in deaerated solution, and two forms in oxygenated- N_2O solution. Although the composition of these forms becomes insensitive to dose in the plateau region, radical-induced changes may occur on other sites of the hemoprotein that are not monitored by the analysis method employed. The plateau region is thus not a steady state for the entire myoglobin molecule; it may nevertheless be considered as such for the prosthetic group in this low dose range. It is important, furthermore, to note that the steady states addressed in these analyses are those induced by radiolysis only. Prolonged radiolysis over time will, however, produce different plateau compositions due to the inclusion of the thermal ferriMb regeneration process in the scheme of reactions. Consequently, the compositions attained without allowance for postirradiation effects will depend on the dose-rate of the γ -source.

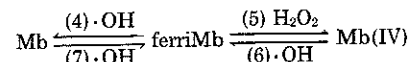
The observed reactions in N_2O -saturated solution are:



where the G_4 and G_5 values, estimated in the limit of zero dose, are about 1.4 and 0.7, respectively. The G_5 value is consistent with H_2O_2 being the reagent responsible for reaction 5. Van Leeuwen *et al.* (8) claim an analogous G_4 value of ~ 0.05 . We attribute this large discrepancy to the inadequate separation of the radiation-induced and thermal regeneration effects in the previous study. Indeed, we obtain a G value of ~ 0.05 for a thermally equilibrated $31 \mu\text{M}$ ferriMb solution γ -irradiated with 5.5 krad. Clearly comparison of G values in myoglobin radiolysis systems is only meaningful if both the radiolysis dose and the time elapsed between the radiolysis and subsequent analysis are given. As written, the ferriMb \rightarrow ferriperoxide conversion is accountable by H_2O_2 reactivity with no significant direct or indirect involvement of precursor $\cdot\text{OH}$ radicals; this feature will be qualified later in the discussion. Since reactions 4 to 6 do not constitute a steady state condition, another process, specifically:



must also participate in the radiolysis system. This process is presumably driven by $\cdot\text{OH}$ radicals. Consequently, the steady state scheme takes the following overall form:



Estimates of the G values of reactions 6 and 7 can be derived from the known G values and the steady state composition. For the Mb and Mb(IV) percentages to remain constant with increasing dose in the plateau region, both $G_7[\text{Mb}] \approx G_4[\text{ferriMb}]$ and $G_6[\text{Mb(IV)}] \approx G_5[\text{ferriMb}]$. Substitution of the relevant data gives $G_6 \approx 0.8$ and $G_7 \approx 3.4$.

As shown by the chromatographic product analyses, dimer material and (by stoichiometric inference) globin disproportionation products account for the remainder of the $\cdot\text{OH}$ radical reactivity with ferriMb. In the moderate-dose plateau region, bimolecular processes function as a major sink for the $\cdot\text{OH}$, thereby leading to a progressive depletion of unmodified globin with increasing dose. Maintenance of the steady state,

TABLE IV
Radical-induced conversion efficiencies among myoglobin
prosthetic groups in deaerated solution at pH 7.3

Radical	Conversion	G value	Efficiency ^a
·OH, H·	FerriMb → Mb	1.4	0.23 ^b
·OH, H·	Mb(IV) → FerriMb	0.8	0.13 ^c
·OH, H·	Mb → FerriMb	3.4	0.55 ^c
e _{aq} ⁻ , H·	FerriMb → Mb	1.6	0.47 ^b
e _{aq} ⁻ , H·	Mb(IV) → FerriMb	0.8	0.24 ^c
e _{aq} ⁻ , H·	Mb → FerriMb	0.6	0.18 ^c

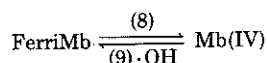
^a Taken as $G(\text{conversion})/G(\text{radical})$, where $G(\cdot\text{OH}, \text{H}\cdot) = 6.2$ and $G(e_{\text{aq}}^-, \text{H}\cdot) = 3.4$.

^b Measured value.

^c Derived value.

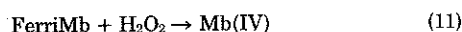
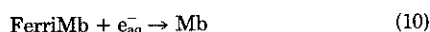
therefore, requires the mechanisms of prosthetic group interchange to be insensitive to these chemical changes on the hemoprotein structure. At high doses, degradation of the heme group may occur, disrupting the steady state condition, and ultimately generating green myoglobin derivatives (12, 16).

In the presence of oxygen the ·OH radical system attains a two-component steady state condition of the form:



where $G_8 \approx 1.5$ in the zero dose limit. As will be discussed in the next section, reaction 8 is driven by both H_2O_2 and ·OH. Given that $G_8[\text{ferriMb}] = G_9[\text{Mb(IV)}]$ in the plateau region, we derive $G_9 \approx 0.7$ from the steady state composition data.

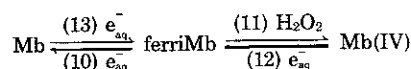
The steady state condition attained in the ferriMb + e_{aq}⁻ system can be interpreted in the same way, based on the following observed reactions:



where $G_{10} \approx 1.6$ and $G_{11} \approx 0.4$ in the zero dose limit. The G_{11} value is significantly lower than the analogous G_5 value in the ·OH radical system. This lower peroxide yield may result, in part, from competition for the H_2O_2 by e_{aq}⁻, for which $k(e_{\text{aq}}^- + \text{H}_2\text{O}_2) \approx 2 \times 10^{10} \text{ M}^{-1}\text{s}^{-1}$ (29), compared with $k(\cdot\text{OH} + \text{H}_2\text{O}_2) \approx 2 \times 10^7 \text{ M}^{-1}\text{s}^{-1}$ (30). The condition of radiolysis steady state among the prosthetic forms requires the participation of reaction 13. In addition to possible H_2O_2 participation, this reaction may involve e_{aq}⁻, a



feature which will be discussed later. The steady state scheme is therefore:



Proceeding as before, we derive $G_{12} \approx 0.8$ and $G_{13} \approx 0.6$. Although not specifically analyzed in this case, it can be presumed, by analogy to the ·OH system, that bimolecular processes involving hemoprotein radical sites not involved in redox on the prosthetic group behave as the reactive sinks of e_{aq}⁻ attack in the plateau region.

Product Evaluation—Our spectral analyses clearly show that both Mb and ferriperoxide are formed upon radiolysis of ferriMb in the absence of oxygen. Subsequent aeration leads to quantitative Mb → MbO₂ conversion, and a product mixture of MbO₂ and the peroxide consequently results. In radiolyses in the presence of air, we have shown that production

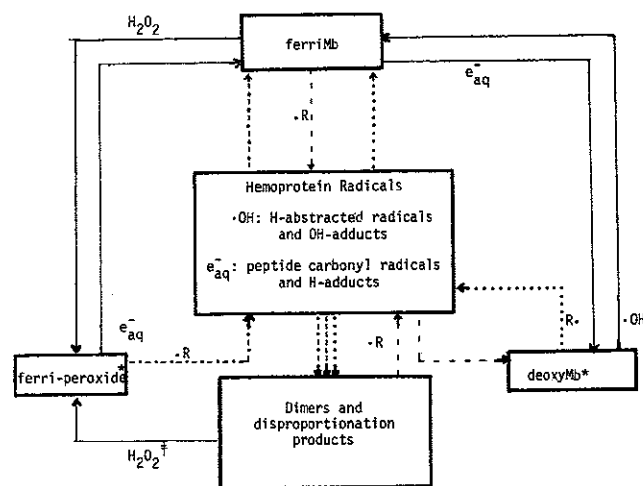
of the ferriperoxide predominates. The qualitative spectral data obtained by Satterlee *et al.* (17) for ferriMb radiolysis under deaerated and oxygenated conditions are fully consistent with our observations. The various interpretations of the product spectra reported in earlier studies (10–17, 20) are a consequence of the unconsidered features addressed in this investigation.

The maintenance of ferriMb → Mb reduction in the presence of ·OH-scavenging *tert*-butyl alcohol led Satterlee *et al.* (17) to conclude that this conversion was a consequence of e_{aq}⁻ reactivity. This conclusion refuted earlier proposals (10, 14) that ·OH radical was the dominant initiator of the conversion process. Our results show that both ·OH and e_{aq}⁻ initiate not only this conversion, but also a series of one-equivalent processes involving the Mb(II), Mb(III), and Mb(IV) formal redox states, albeit with different efficiencies.

Globin-mediated Mechanisms—The measured and derived radical-induced conversion efficiencies among the prosthetic group forms are shown in Table IV. Interpretation of these efficiencies requires some background on the nature of radical attack on the myoglobin substrate.

In myoglobin, the ferriheme is completely buried, except for one edge, in a pocket formed by 8 helices folding back upon themselves (31). The reaction of free radicals with ferriMb, therefore, would be a composite of attack on the exposed globin and directly into the ferriheme pocket. The dispersion of free radical reactivity over the macromolecule is dependent both on the number, spatial disposition, and kinetic reactivity of constituent peptide sites and on the accessibility of the buried prosthetic group. The nature of the reactive sites can be reasonably deduced from established reactivity patterns of radical attack on amino acids and simple peptides (32, 33), and from knowledge of the residue content of the myoglobin. It is known that sites of particular importance for acceptance of e_{aq}⁻ are aromatic and heterocyclic groups and the peptide carbonyls; the carbonyl sites are clearly ubiquitous over the globin structure. Similarly, ·OH and H· add readily to ring residues and, with lower reactivity, abstract H atoms from CH (and NH) sites.

It is known that carbon-centered abstracted radicals possess



·R = ·OH, e_{aq}⁻

ferri-peroxide → ferriMb + modified globin

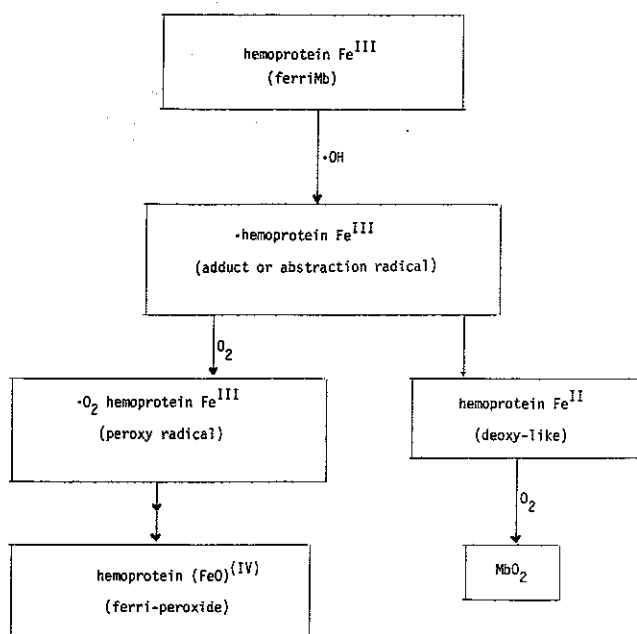
ferriMb → deoxyMb + modified globin

deoxyMb → ferriMb + modified globin

* general designation for unmodified, dimer, and oxidized globin material

† applicable to modified ferriMb material

SCHEME 1



SCHEME 2

reducing ability (2). In addition, the potential for reattainment of resonance stabilization probably imparts mild oxidizing ability to solvated OH adducts of phenylalanine, tyrosine, and tryptophan (34). The e_{aq}^- -adduct to the heme group of deoxymyoglobin may exhibit an oxidizing influence with respect to Fe-centered redox through a concerted process involving overall reduction at a site near the prosthetic group. Indirect e_{aq}^- -induced oxidation of cytochrome(II) *c* to the ferri form is known, in which a thioether bond linking the heme to the protein is reductively cleaved (35). The process involves the transfer of two reducing equivalents to the thioether bond, one each being obtained from the Fe(II)/Fe(III) and porphyrin-adduct/porphyrin couples. Although a readily reducible thioether site is not available in the myoglobin structure, this metalloprotein has a compensating larger thermodynamic drive for Fe(II) \rightarrow Fe(III) oxidation by ~ 0.2 V compared with the cytochrome (8). Without offering mechanistic detail, we propose that e_{aq}^- adducts to the heme group may participate as one component of a 2-eq redox process in which Mb \rightarrow (modified) ferriMb conversion results. Insignificant oxidative involvement of adduct radicals in the observed ferriMb \rightarrow ferriperoxide conversion would be expected, since only strong oxidants with reduction potentials ≥ 0.9 V are capable of driving this process (26).

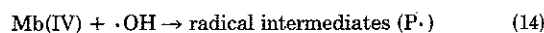
Since there is no driving force for \cdot OH attack at the iron center of ferriMb, and metal-centered reduction is an unlikely result of \cdot OH + hemin(III) (2) reactivity, the observed 23% reduction efficiency of ferriMb \rightarrow Mb indicates the participation of protein-mediated reductive transfer in this process. The formation of dimers and evidence of second order transient kinetics are both consistent with bimolecular combination of \cdot OH-generated globin radicals. However, the reductive and bimolecular modes of globin radical decay do not directly compete, as evidenced by the observed independence of the reduction and dimerization yields on dose-rate over the enormous experimental dose-rate variation. Radical sites initiating reductive transfer are, therefore, reactively distinguishable from other sites decaying bimolecularly. This reactive duality may relate both to differences in radical identity (adduct radical *versus* abstraction radical) and to the structural disposition of the radical site on the globin. This feature is also evident from the dose-rate independence of e_{aq}^- -induced

ferriMb \rightarrow Mb conversion. In this case, globin radical differences may relate to peptide carbonyl and ring adduct sites, in addition to structural considerations. The value we obtain of 47% for the efficiency of e_{aq}^- -induced ferriMb \rightarrow Mb conversion is somewhat less than previously reported values of $\sim 70\%$ (4, 6). Given the dispersed reactivity of e_{aq}^- over the entire metalloprotein, our value is nevertheless too high to be solely accountable by direct interaction at the heme group, and is consistent, therefore, with some participation of protein-mediated redox transfer. For the 1-eq redox processes listed in Table IV, it is clear that \cdot OH demonstrates better oxidizing efficiency than e_{aq}^- , whereas e_{aq}^- exhibits better reducing efficiency than \cdot OH. These reactivity trends are consistent with there being some direct interaction of these primary radicals with the iron center, inasmuch as \cdot OH is a strong oxidant and e_{aq}^- is a strong reductant in electron transfer processes. For the purpose of summary, the proposed mechanism of free radical interactions with myoglobin in deaerated solution is shown in Scheme 1 in which direct and protein-mediated redox processes are included.

The value of $G(\text{Mb(IV)}) \approx 1.5$ obtained in the zero dose limit for radiolysis in the presence of $\text{N}_2\text{O-O}_2$ mixtures is too high to be solely accountable by the reaction of ferriMb with H_2O_2 for which $G_5 \approx 0.7$ in the same limit. The generation of ferriperoxide by this latter reaction is known to evolve oxygen (27); it is most unlikely, therefore, that an initial presence of O_2 would change the reaction stoichiometry. In addition to this mechanistic feature, there is no MbO_2 generated under these oxygenated conditions. Taken together, these results suggest that extra ferriperoxide generated in the presence of O_2 may result from a diversion of intermediate reactivity away from reductive conversion toward peroxide production. Thus, the \cdot OH-induced ferriMb \rightarrow Mb and ferriMb \rightarrow ferriperoxide conversions apparently derive from common globin radical precursors. In the presence of O_2 , those globin radicals capable of reductive conversion to Mb are scavenged to generate, ultimately, the peroxide; this is illustrated in Scheme 2 in which peroxy radical intermediacy is presumed (36).

A possible source of the extra ferriperoxide may be from HO_2/O_2^- radicals formed through the decomposition of alkylperoxy radicals on the globin moiety (37), in addition to those formed by O_2 reaction with H atoms. In a separate study (38), O_2^- radicals have been shown to react slowly with ferriHb to generate a product which, from its spectral properties in the Soret region, is proposed to be HbO_2 . Consistent with the difficulties encountered in the identification of the absorbing product in the $\text{O}_2^- + \text{ferriHb}$ reaction, it is possible that the product is actually the ferriperoxide derivative, having spectral similarity to the oxy form. We tentatively propose, therefore, that the \cdot OH-induced ferriMb \rightarrow ferriperoxide conversion in $\text{N}_2\text{O/O}_2$ solution, for which $G \approx (G_8 - G_6)$, may involve the following sequence of steps: globin peroxy radical $\rightarrow \text{HO}_2 \cdot \rightarrow$ ferriperoxide. Comparison of this G value with $G_4 \approx 1.4$ suggests that $\sim 60\%$ of the globin radicals initiating reductive transfer to generate Mb in the absence of O_2 are redirected to ferriperoxide formation by O_2 scavenging.

The similarity of the G_8 and G_9 values, which reflect the conversion efficiencies of the ferriperoxide \rightarrow ferriMb process in the absence and presence of O_2 , respectively, may be explained in one of two ways. Common to both alternatives is the preliminary reaction 14. The apparent independence of the ferriMb yield on O_2 may result from a fast protein-mediated 1-eq transfer process, with which O_2 -scavenging cannot compete.



That is,



for which $k_{15} \gg k_{16} [O_2]$. With $k_{16} \sim 10^9 \text{ M}^{-1} \text{ s}^{-1}$ (38), this explanation requires $k_{15} > 10^6 \text{ s}^{-1}$; this facility of transfer may derive from the high driving force of the ferriperoxide/ferriMb couple (8). Alternatively, if $k_{15} \leq k_{16} [O_2]$, the similarity of G_6 and G_9 may result from reaction 17



wherein the overall efficiency of ferriMb production remains unchanged after the route of peroxy intermediacy is taken. Again, the high reduction potential for the ferriperoxide/ferriMb couple may drive this process; k_{17} may be significantly less than k_{15} , however. In contrast to the reduction of ferriperoxide by $\cdot\text{OH}$, the course of the analogous ferriMb reduction is markedly altered by the presence of O_2 . This feature clearly suggests that the 1-eq transfer rate from radical sites on ferriMb is competitive with O_2 -scavenging, for which the rate constant, as for k_{16} is $\sim 10^9 \text{ M}^{-1} \text{ s}^{-1}$. In such a case, an intramolecular transfer rate constant of $\leq 10^5 \text{ s}^{-1}$ is implied for the ferriMb \rightarrow Mb reduction. This process was not directly discernible in accessible wavelength regions by pulse radiolysis, however.

Although a tunneling mechanism has been proposed from remote radical sites to the iron center in the cytochrome(III) $c + \cdot\text{OH}$ system (39), the alternative path of fast consecutive intramolecular steps could not be excluded. Supportive of this latter "chemical transfer" mechanism is the mounting evidence for a highly dynamic nature of the myoglobin structure (40). Modification of radical spin-density distributions by orbital overlap within the dynamic macromolecule may account for efficient intramolecular redox transfer to the iron center. Aspects of this have been demonstrated in model systems having separated donor and acceptor sites (41). Studies at shorter time resolution and in frozen media may clarify the nature of the transfer process.

REFERENCES

- Shafferman, A., and Stein, G. (1975) *Biochim. Biophys. Acta* **416**, 287
- Simic, M. G., and Taub, I. A. (1978) *Faraday Discuss. Chem. Soc.* **63**, 207
- Land, E. J., and Swallow, A. J. (1974) *Biochim. Biophys. Acta* **368**, 86
- Wilting, J., Braams, R., Nauta, H., and Van Buuren, K. J. H. (1972) *Biochim. Biophys. Acta* **283**, 543
- Clement, J. R., Lee, N. T., Klapper, M. H., and Dorfman, L. M. (1976) *J. Biol. Chem.* **251**, 2077
- Ilan, Y. A., Rabani, J., and Czapski, G. (1976) *Biochim. Biophys. Acta* **446**, 277
- Wilting, J., Raap, A., Braams, R., De Bruin, S. H., Rollema, H. S., and Janssen, L. H. M. (1974) *J. Biol. Chem.* **249**, 6325
- Van Leeuwen, J. W., Tromp, J., and Nauta, H. (1979) *Biochim. Biophys. Acta* **577**, 394
- Land, E. J., and Swallow, A. J. (1971) *Arch. Biochem. Biophys.* **145**, 365
- Tappel, A. L. (1956) *Food Res.* **21**, 650
- Brown, W. D., and Akoyunoglou, J.-H. A. (1964) *Arch. Biochem. Biophys.* **107**, 239
- Ginger, I. D., Lewis, U. J., and Schweigert, B. S. (1955) *J. Agric. Food Chem.* **3**, 156
- Clarke, R., and Richards, J. F. (1971) *J. Agric. Food Chem.* **19**, 170
- Bernofsky, C., Fox, J. B., Jr., and Schweigert, B. S. (1959) *Arch. Biochem. Biophys.* **80**, 9
- Satterlee, L. D., Brown, W. D., and Lycometros, C. (1972) *J. Food Sci.* **37**, 213
- Kamarei, A. R., Karel, M., and Wierbicki, E. (1979) *J. Food Sci.* **44**, 25
- Satterlee, L. D., Wilhelm, M. S., and Barnhart, H. M. (1971) *J. Food Sci.* **36**, 549
- George, P., and Irvine, D. H. (1952) *Biochem. J.* **52**, 511
- Fox, J. B., Jr., Nicholas, R. A., Ackerman, S. A., and Swift, C. E. (1974) *Biochemistry* **13**, 5178
- Giddings, G. G., and Markakis, P. (1972) *J. Food Sci.* **37**, 361
- Lycometros, C., and Brown, W. D. (1973) *J. Food Sci.* **38**, 972
- Shieh, J. J., Sellers, R. M., Hoffman, M. Z., and Taub, I. A. (1979) in *Radiation Biology and Chemistry: Research Developments* (Edwards, H. E., Navaratnam, S., Parsons, B. J., and Phillips, G. O., eds) pp. 179-188, Elsevier, Amsterdam
- Hardman, K. D., Eylar, E. H., Ray, D. K., Banaszak, L. J., and Gurd, F. R. N. (1966) *J. Biol. Chem.* **241**, 432
- Yamazaki, I., Yokota, K., and Shikama, K. (1964) *J. Biol. Chem.* **239**, 4151
- Davis, B. J. (1964) *Ann. N. Y. Acad. Sci.* **121**, 404
- George, P. and Irvine, D. H. (1953) *Biochem. J.* **53**, XXV
- King, N. K., and Winfield, M. E. (1963) *J. Biol. Chem.* **238**, 1520
- Simic, M., Neta, P., and Hayon, E. (1969) *J. Phys. Chem.* **73**, 3794
- Anbar, M., Bambeneck, M., and Ross, A. B. (1972) *National Stand. Ref. Data Series, National Bureau Standard No. 43*
- Farhataziz, and Ross, A. B. (1977) *National Stand. Ref. Data Series, National Bureau Standard No. 59*
- Dickerson, R. E., and Geis, I. (1969) *The Structure and Action of Proteins* p. 49, Harper and Row, New York
- Simic, M. G. (1978) *J. Agric. Food Chem.* **26**, 6
- Taub, I. A., Halliday, J. W., and Sevilla, M. D. (1979) *Adv. Chem. Ser.* **180**, 109
- Bansal, K. M., and Henglein, A. (1974) *J. Phys. Chem.* **78**, 160
- Butler, J., De Kok, J., De Wille, J. R., Koppenol, W. H., and Braams, R. (1977) *Biochim. Biophys. Acta* **459**, 207
- Howard, J. A. (1973) in *Free Radicals* (Kochi, J. K., ed) Vol. 2 p. 3, Wiley-Interscience, New York
- Ilan, Y., Rabani, J., and Henglein, A. (1976) *J. Phys. Chem.* **80**, 1558
- Ferradini, C., Foos, J., Gilles, L., Haristoy, D., and Pucheault, J. (1978) *Photochem. Photobiol.* **28**, 851
- Van Leeuwen, J. W., Raap, A., Koppenol, W. H., and Nauta, H. (1978) *Biochim. Biophys. Acta* **503**, 1
- Frauenfelder, H., Petsko, G. A., and Tsernoglou, D. (1979) *Nature* **280**, 558
- Whitburn, K. D., Hoffman, M. Z., Simic, M. G., and Brezniak, N. V. (1980) *Inorg. Chem.* **19**, 3180